Thermodynamic Functions of Concentrated Protein Solutions from Phase Equilibria

Dimiter N. Petsev,[†] Xioxia Wu,[‡] Oleg Galkin,[†] and Peter G. Vekilov*[,†]

Department of Chemical Engineering, University of Houston, Houston, Texas 77204-4004, and Department of Chemistry, University of Alabama in Huntsville, Huntsville, Alabama 35899

Received: December 26, 2002; In Final Form: February 15, 2003

For insight into the thermodynamics and phase behavior in concentrated protein solutions, we study the liquid−liquid phase separation with lysozyme. We determine independently the binodal and spinodal lines, and the second virial coefficient of the protein at $275 < T < 295$ K. From these data, we determine the protein chemical potential and osmotic pressure for concentrations as high as 320 mg mL^{-1} in the above temperature range. We find that for this protein, the enthalpy of the liquid−liquid separation vanishes at the critical temperature, T_c, and is comparable to and may exceed the crystallization enthalpy (∼65 kJ mol^{-1}) at lower Ts. The enthalpy of the pair interactions averaged over all polar angles is significantly lower; this comparison suggests structuring of the dense liquid. We propose that the pair of parameters (molecular volume, second virial coefficient) may be an adequate predictor of the phase behavior of solutions of proteins with relatively simple interaction potentials.

Introduction

The native environments in which proteins function are far from ideal solutions. The total protein concentration in the cytoplasm reaches up to 350 mg mL^{-1},[1] corresponding to average separations of <10 Å between the molecular surfaces.[2] The short separations enhance the interactions between the molecules: specific binding, electrostatic, hydrophobic, and interactions involving solvent structuring.[3−6] The interactions severely modify the proteins' chemical potential and activity[7,8] and affect their conformational stability.[9,10] Thus, the total protein concentration as well as the segregation and selection of a group of proteins in a particular area of the intracellular space may be an important means of regulation of the protein stability and function.

Protein intermolecular interactions and their effects on protein activity and chemical potential have been studied at relatively low concentrations employing a variety of scattering techniques.[11−13] An alternative probe utilizes the fact that the interactions underlie the phase behavior of the solutions (see, e.g., ref 14). The liquid−liquid (L−L) phase separation that occurs in concentrated protein solutions[15−17] is particularly suitable, because (i) since both phases are aqueous solutions, a single standard state can be defined;[18] and (ii) the coexistence boundary is typically a single smooth curve with a critical point.[19]

Aside from the insight into the thermodynamics of the concentrated protein solutions that it provides, the L−L phase separation is of interest as a fundamental biological phenomenon and a pathway of biological organization.[20,21] It has been hypothesized that liquid−liquid separation occurs in the cytoplasm[22,23] and underlies the organization of the cytoplasmic space unseparated by membranes.[20,21] Furthermore, the L−L separation has been put forth as a prerequisite for the formation of protein solid phases: polymers, crystals, etc.[16,24−26] The formation of protein solid phases is the primary pathogenic event in diseases ranging from the sickle cell anemia[27] and eye cataracts,[28] to Alzheimer's, Huntington's, and the prion diseases and other neurological disorders.[29,30]

Thus, data on the thermodynamics on the L−L separation (i) provide quantitative insight into the forces that drive the phase behavior in protein solutions, and (ii) allow determination of the protein activity in concentrated solutions and analysis of the factors that affect the activity. The goals of the investigations reported here are to obtain such data for a model protein and develop a general method for the interpretation of data on the phase behavior. We chose lysozyme from hen egg white because of its ready availability in a relatively pure state and the huge base of data on this protein.

In protein solution, the dense liquid phase is metastable[24,31] and over time decays into a solid phase: crystals, polymers, aggregates, etc. However, with lysozyme, crystal formation is slow, the dense liquid is preserved over several days, and L−L separation can be reversed and reestablished repeatedly without hysteresis.[26] Thus, in the discussion below, we view the dense liquid phase as stable and the L−L equilibrium as a final state of the solution.

Methods

Solutions. We used 6× crystallized lysozyme from Seikagaku. To prepare solutions of concentration below 110−120 mg mL^{-1}, the protein was dissolved in 50 mM NaAc buffer, and NaCl solution in the same buffer was added to a final 4% (w/v) concentration of the salt. To obtain protein concentrations between 90 and 320 mg mL^{-1}, the above solution was cooled to achieve L−L phase separation. After centrifugation, the dense phase was collected and used after a concentration determination. As shown in ref 16, the acetate buffer and NaCl do not segregate between the two liquid phases. In the concentration range where the two methods of solution preparation overlap, identical results were obtained.

Determination of the Binodal and Spinodal, and the Second Virial Coefficient. A solution sample of known concentration was filtered and placed in a quartz cuvette held

[†] University of Houston.
[‡] University of Alabama in Huntsville.

10.1021/jp0278317 CCC: $25.00
Published on Web 03/29/2003

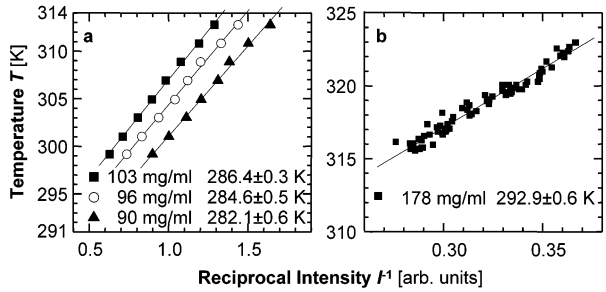

Figure 1. Illustration of determination of the spinodal. Plots of the temperature T versus the reciprocal value of the intensity I scattered at 90°. Different symbols indicate different protein concentrations as indicated in the legends. (a) At protein concentrations $C < 120$ mg mL^{-1}, the average of ~20 intensity values recorded at the respective T are plotted; (b) at $C > 90$ mg mL^{-1}, all intensity values recorded as T was lowered at a rate of ~0.2 °C min^{-1} are plotted. The temperatures at which the extrapolated I^{-1} reaches 0 were taken as the spinodal temperatures and are shown for each protein concentration.

in a thermostated enclosure ($\Delta T < 0.1$ K) in the goniometer of a Brookhaven static and dynamic light-scattering setup.[32,33] Laser light ($\lambda = 632.8$ nm) intensities transmitted and scattered at 90° were monitored. Because of the small molecular diameter of lysozyme, $a \sim 3$ nm, at all scattering angles between 0 and 180°, the product $qa < 0.05$ (q − wave vector). Thus, the lengthscales, which we probe, are $\gg a$, and the data reflect the behavior of large numbers of molecules. Accordingly, no meaningful angular dependence of the scattered intensity is observed.[6]

A determination started at a temperature higher than the expected binodal but lower than 318−321 K (45−48 °C), above which the protein might denature. At protein concentrations below 100−110 mg mL^{-1}, at which the onset of crystallization is slow, the temperature was lowered in 1 or 2 K steps. At each step, equilibration of the solution, judged by the scattered intensity fluctuating around a steady value, was achieved after ~1−2 min. To determine the spinodal temperature, as in ref 14, the mean (of ~20 records) reciprocal scattered intensity was plotted as a function of temperature, as in Figure 1a. The spinodal temperature was determined as the point at which the extrapolated line through the data intersects the temperature axis. Note that the determination of spinodal points below 270 K involves such extrapolations over ~15 K and more; hence, these points were not used in data fitting. At higher protein concentrations, temperature was lowered at a steady rate of 0.2 °C min^{-1}, and the actual temperature and the scattered intensity were recorded at 30-s intervals, as shown in Figure 1b.

The binodal temperature was determined by the disappearance of the light spot behind the sample as a result of the sudden increase of the sample turbidity after the formation of dense-phase droplets. Alternatively, drops of 1−5 μL of solution were observed under the microscope as the temperature was lowered in 1−2-K steps. Clouding of the solution at a certain temperature was unambiguously detectable.[34] With both methods, reversibility and reproducibility were verified by repeated observations at the last several temperature steps. The data on the binodal and spinodal in Figure 2 are limited at a protein concentration of ~320 mg mL^{-1}, above which rapid crystallization and gelation prevent all three types of determinations.

The second virial coefficient was measured at 16 temperatures in the range 278−293 K, Figure 3. We employed static light scattering[33,35] and linear Debye plots at each temperature. The concentration of the test solutions was varied between 15 and 40 mg mL^{-1} in the single-phase region for the respective temperature where the protein is monomeric and monodisperse.

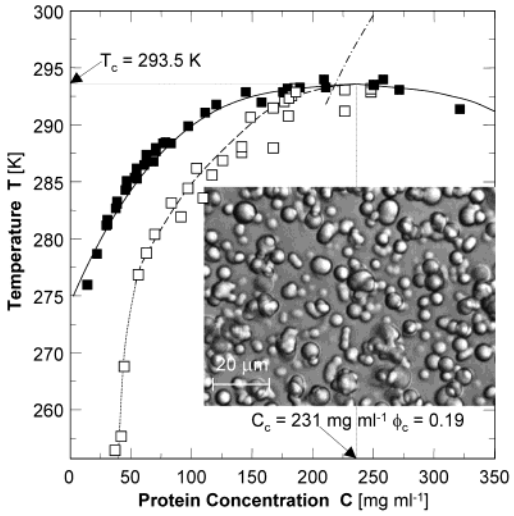

Figure 2. A section of the phase diagram, containing the liquid−liquid-phase separation, of a lysozyme solution in 0.05 M sodium acetate buffer with pH 4.5 and with 4% NaCl. Solid symbols, the coexistence line, binodal; open symbols, the spinodal for the liquid−liquid-phase separation. The critical temperature and concentration, T_c and C_c, and the critical volume fraction ϕ_c are indicated in the plot: (—) fit to binodal using eq 1; (---) spinodal calculated using eq 7; (•••) guide to the eye for spinodal points at low temperatures; (— • — • —) approximate location of gelation line according to ref 16. Insert: droplets of high-density liquid that appear in a 95 mg mL^{-1} lysozyme solution at 288 K. Since the corresponding composition of the dense phase is below the gelation line, many of the droplets do not coalesce.

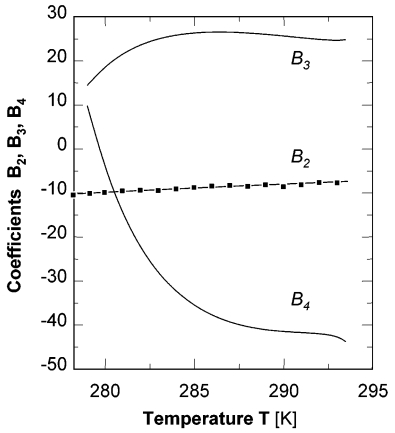

Figure 3. The dependence of the osmotic virial coefficients B_2, B_3, and B_4 on temperature. B_2 was directly determined by static light scattering; B_3 and B_4 were calculated from the liquid−liquid binodal data, as discussed in the text.

Results

Phase Diagram. As shown in ref 16, the liquid−liquid coexistence lines $T_{L-L}(C)$ for lysozyme solutions fit well the function,

$$T_{L-L} = T^{crit}\left\{1 - A\left|\frac{C^{crit} - C}{C^{crit}}\right|^{1/\beta}\right\} \qquad (1)$$

even at concentrations significantly higher than those probed in Figure 2. In eq 1, T^{crit} and C^{crit} are, respectively, the critical temperature and lysozyme concentration; β is the critical exponent; and A is an amplitude.[16] From the data in Figure 2, $T^{crit} = 293.5$ K and $C^{crit} = 231$ mg mL^{-1}; the best-fit values for β and A^{L-L} for the binodal are $\beta^{L-L} = 0.325$ and $A^{L-L} = 0.0735$, as in ref 16. For the spinodal, we use the same relation

and get $\beta^{sp} = 0.48 \pm 0.05$ and $A^{sp} = 0.089 \pm 0.007$, that is, $A^{sp}/A^{L-L} \approx 1.21$. The concentration in Figure 2 is easily converted to volume fraction, $\phi = C\upsilon_p N_A/M_w$, where $M_w = 14\,500$ g mol^{-1} is the molecular mass of lysozyme and $\upsilon_p = 2.0 \times 10^{-20}$ cm^3 is the molecular volume in solution.[36,37] Thus, $\phi^{crit} = 0.190$.

The liquidus (solubility) lines of the tetragonal and orthogonal crystals of lysozyme are monotonic and pass through $T \sim 313-333$ K at concentrations $\sim 10-50$ mg mL^{-1},[38,39] well above the L−L coexistence line. In further agreement with previous findings, solutions for which $C \geq 230$ mg mL^{-1} gel.[16,26]

Chemical Potential of the Protein. We derive an expression for the chemical potential of the protein in the solution as a function of the protein concentration. We use the fact that at constant temperature, the mechanical and chemical equilibria between the low L and the high H density phases require equality of the osmotic pressures, Π, and of the chemical potentials of the protein in the two phases, μ.

$$\mu_L = \mu_H, \Pi_L = \Pi_H \quad (2)$$

Some mean-field approaches, such as the Flory−Higgins or van der Waals theories, predict $\beta^{L-L} = \beta^{sp} = 0.5$ and $A^{sp}/A^{L-L} = \sqrt{3} \cong 1.71$.[40] The different β^{L-L} and A^{sp}/A^{L-L} found above indicate that the lysozyme solutions are poorly described in terms of these theories. Hence, we use a virial-type expression, in which the virial-type coefficients are allowed to vary with temperature, yet no assumptions on the concrete temperature dependence are made. Since the water, NaCl, and $NaCH_3COO$/CH_3COO buffer are not segregated between the two phases,[16] we approximate the solution with a single-component two-phase system. In each phase and at each temperature, T,

$$\frac{\Pi \upsilon_p}{k_B T} = \frac{\phi(1 + \phi + \phi^2 - \phi^3)}{(1 - \phi^3)} + B_2'\phi^2 + B_3'\phi^3 + B_4'\phi^4 \quad (3)$$

and

$$\frac{\mu - \mu^\circ}{k_B T} = \ln \phi - 3 + \frac{(3 - \phi)}{(1 - \phi)^3} + 2B_2'\phi + \frac{3}{2}B_3'\phi^2 + \frac{4}{3}B_4'\phi^3 \quad (4)$$

where μ° is an integration constant. In eqs 3 and 4, the effective repulsion due to the excluded volume of the protein molecules, "hard-spheres repulsion", is accounted for by the Carnahan−Starling expressions (CS),[41] constituting the terms not containing B_i' on the right side of eqs 3 and 4 These B_i''s account for all other interactions[42] so that the total B_i's are

$$B_i = B_i^{hs} + B_i' \quad i = 2, 3, 4 \quad (5)$$

Although the CS terms in eqs 3 and 4 are an exact representation of μ and Π for noninteracting hard spheres, the correction terms are limited to those containing B_2, B_3, and B_4, not because we know that the fifth order term is small. Our reason is that at each temperature, we have three independent determinations: ϕ_L and ϕ_H from Figure 2 and B_2 from Figure 3.

Equations 3 and 4 are linked by another form of the Gibbs−Duhem equation for a single component systems at constant temperature exhibiting osmotic pressure.

$$\mu = \upsilon_p \int (\partial\Pi/\partial\phi)/\phi \, d\phi \quad (6)$$

An expression similar to eq 4 was used to relate the protein chemical potential and concentration stemming from Monte Carlo simulations.[42]

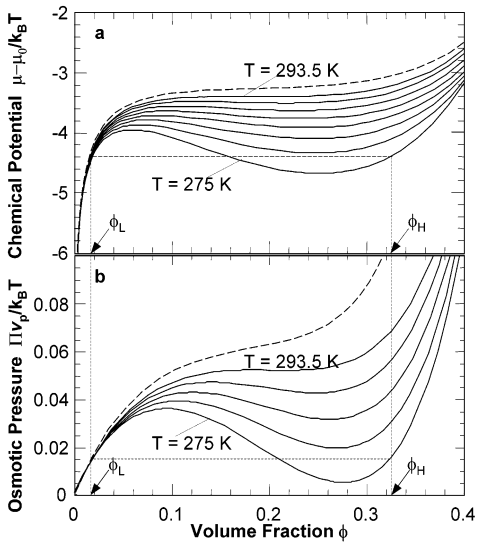

Figure 4. Dependencies of (a) the chemical potential μ and (b) osmotic pressure Π on the volume fractions ϕ at different temperatures. The top solid lines in both plots were calculated at the critical point ($T =$ 293.5 K); the others, at 290, 285, 280, and 275 K, respectively, as discussed in the text; (− − −) are extrapolations for $T = 295$ K $> T_c$, calculated as discussed in the text.

The temperature dependencies of the coefficients B_3, and B_4, resulting from the joint solution of eqs 3 and 4 in the temperature range probed by the L−L separation are shown in Figure 3. The corresponding dependencies of the osmotic pressure Π and the chemical potential μ on the protein volume fraction ϕ, calculated using eqs 3 and 4 are shown in Figure 4.

As a consistency check, one might use the $\mu(\phi)$ dependencies in Figure 4a to calculate the spinodal points at each temperature as ϕ's, for which

$$(\partial\mu/\partial\phi)_T = 0 \quad (7)$$

Indeed, Figure 2 shows that the calculated spinodal points agree reasonably well with the experimentally determined ones. However, as shown in the discussion below, because of the ambiguity in the definition of the spinodal,[43] this correspondence should not be awarded undue significance. For the same reason, attempts to use the pair of ϕ's at the spinodal to obtain the fifth and sixth order terms in eqs 3 and 4 would be unjustified.

Figure 4 also shows that by extrapolating the dependencies $B_i(T)$ from Figure 3 to temperatures higher than T^{crit}, one can obtain $\mu(\phi)$ even at temperatures at which L−L separation does not occur. Since $B_i(T)$ may be nonlinear functions, such extrapolations cannot cover wide temperature ranges.

Discussion

Spinodal and the Metastability−Instability Boundary. We address here the stability of a single-phase solution quenched below the L−L coexistence line. In such a solution, the spinodal is defined as the boundary between the metastable state, where a thermodynamic barrier delays the generation of the dense phase, and the unstable state, where the barrier vanishes and the generation of the second phase is controlled only by its growth kinetics.[44] In the mean field approaches, this definition leads to condition 7. It has been pointed out that the mean field approaches are adequate only for systems with very weak and very long-range interactions[43] or at temperatures far below T_c.

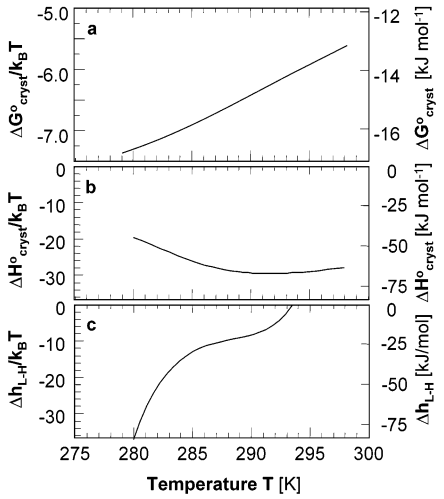

Figure 5. Thermodynamic characteristics of the phase transitions in the lysozyme solutions: (a) the change of the standard free energy upon crystallization $\Delta G°$ at different temperatures, (b) standard crystallization enthalpy $\Delta H°$ at different temperatures, and (c) the difference in partial molar enthalpy for lysozyme between the high- and low-density phases at different temperatures. Since $\mu_L = \mu_H$, $\Delta h_{L-H}/kT = \Delta s_{L-H}/k$.

The combined criterion for validity of the mean field approximation requires that the interaction range r_0 be scaled with the molecular size, a.

$$(r_0/a)^3(1 - T/T_c)^{1/2} \gg 1 \tag{8}$$

Proteins, for which $r_0/a \sim 0.25$,[12,16,45], are a poor fit at all temperatures. In such non-mean-field systems, the spinodal cannot be unambiguously defined.[43] The reasons underlying the correspondence between the "spinodal points" in Figure 1 and the spinodal calculated using eqs 4 and 7 are unclear to us and could be just a fortuitous coincidence. The predictive power of the spinodal in Figure 2 for the dynamics of the phase separation is a subject to tests.

Standard Free Energy and Enthalpy of Crystallization. The thermodynamics of crystallization of lysozyme is well investigated. Thus, the determination of $\Delta G°$ and $\Delta H°$ from the results discussed above serves not only as a benchmark for comparison with the respective functions for the L−L separation but also as another consistency check. At equilibrium between crystal and solution,

$$G^\circ_{crystal}(T) = G^\circ_{solution}(T) + \tilde{\mu}(T, C_e) \tag{9}$$

where $G^\circ_{crystal}(T)$ is the standard molar free energy of the crystal, $G^\circ_{solution}(T)$ is the molar free energy of the solution in its standard state, and $\tilde{\mu}(T, C_e)$ is the deviation from it.[46] Thus, the change in standard free energy upon crystallization.

$$\Delta G^\circ_{cryst} = \tilde{\mu}(T, C_e) \tag{10}$$

We use eq 4 to calculate ΔG°_{cryst} from the data in Figure 4a with the solubility from refs 39 and 47. The results in Figure 5a show that ΔG°_{cryst} has a weak temperature dependence around -15 kJ mol^{-1}, close to previous determinations in this temperature range.[48,49] The Gibbs−Helmholtz equation[46] allows determination of the standard enthalpy change upon crystallization, ΔH°_{cryst}, shown in Figure 5b. At the high end of the probed temperatures, ΔH°_{cryst} reaches $\sim -$ 65 kJ mol^{-1}, close to the calorimetric determination.[50]

Molar Enthalpy of L−L Separation. Since the chemical potentials of the low- and high-density solutions are defined with respect to the same standard state, $\Delta G^\circ_{L-L} = 0$ and the Gibbs−Helmholtz relation cannot be used to evaluate the enthalpy effect of the L−L separation. Hence, we apply the Clapeyron equation[46] for osmotic pressure to obtain the molar enthalpy of the protein in the each phase $\bar{h}_p$.

$$\left.\frac{d\Pi}{dT}\right|_{binodal} = \frac{\bar{h}_p^H - \bar{h}_p^L}{T v_p\left(\frac{1}{\phi_H} - \frac{1}{\phi_L}\right)} \tag{11}$$

A plot of $\Delta h_{L-H} = \bar{h}_p^H - \bar{h}_p^L$ determined from the $\Pi(T, \phi)$ data in Figure 4b is shown in Figure 5c. Since the other solution components are not segregated upon L−L separation,[16] their partial molar enthalpies in the low-density phase are equal to those in the high-density phase.[40] With this in mind, one can easily show that the Δh_{L-H} is a good estimate for the enthalpy effect of the transfer of one mole of protein from the low- into the high-density phase. As the system approaches the critical point, the Δh_{L-H} becomes 0, since the compositions of the two phases converge. At a few degrees below the critical temperature, the enthalpy of L−L separation is comparable to the crystallization enthalpy.

Anisotropy of the Protein Molecules and Phase Behavior of the Protein Solutions. The surfaces of the protein molecules are often viewed as consisting of patches with different dominant characteristics: charged, polar, hydrophobic, etc. If two molecules are brought together along a line through, for instance, hydrophilic patches, the depth, range, and structure of the intermolecular pair potential will be different from the case of, for example, charged patches.[51] It is thought that in a crystal, the locations of the molecules adjacent to a chosen central molecule are in the deepest minimums of the interaction potential around the surface of the central molecule. The search for crystallization conditions is viewed as a search for an angular distribution of deep minimums compatible with a crystallographic symmetry group. On the other hand, in a liquid, the molecules adjacent to a central molecule are randomly distributed and do not occupy the deepest minimums for long times. If the enthalpies of these two phase transitions are viewed as the sums of the energy released when the molecules are brought into the minimums of their interaction potentials, it follows that $|\Delta H_{cryst}| > |\Delta H_{L-H}|$.

Figure 5 indicates that at $T < 282$ K, $|\Delta H^\circ_{cryst}| < |\Delta H_{L-H}|$. Since the dense liquid phase is metastable with respect to the crystals, $|\Delta G_{L-H}| < |\Delta G^\circ_{cryst}|$. Since for lysozyme under similar conditions, $\Delta S_{cryst} \approx -190$ J mol^{-1}K^{-1},[48] we conclude that the L−L separation proceeds with a greater entropy loss. Indeed, from Figure 5c, with $\Delta\mu_{L-H} = 0$, eq 2, $\Delta h_{L-H} = T\Delta s_{L-H} \sim -(22-38)k_BT$, corresponding to a Δs_{L-H} of $-(180-310)$ J mol^{-1} K^{-1}. It follows that crystallization from the dense liquid should have a positive entropy effect. This should not be viewed as an indication that the crystals are less ordered than the dense liquid; as demonstrated in ref 48, $\Delta S_{cryst} > 0$ is often encountered with proteins as a result of the release of solvent molecules associated with protein molecules in the solution.

We consider three factors that may underlie the above inequality of ΔH°_{cryst} and ΔH_{L-H}:

(i) The interactions that determine the phase behavior of the lysozyme solutions are mostly entropic, such as the hydrophobic attraction, allowing anisotropic free energy of the interactions to coexist with isotropic interaction enthalpy. This explanation contradicts the finding of a negative entropy change in lysozyme crystallization from a low-density solution; i.e, entropy favors molecules in the solution and is not a major contributor to the crystal contacts.[48]

(ii) The dense liquid is structured. As supporting evidence, one may consider the negative entropy of formation of the dense phase and the high viscosity and easy propensity of the dense liquid phases of lysozyme to gel, discussed above.

(iii) The minimums around a lysozyme molecule have comparable depth.

Arguments suggesting that ii is likely valid are presented in the next subsection.

The Intermolecular Interaction Potential. As Figure 3 shows, the coefficients B_2, B_3, and B_4 change with temperature. To test if the temperature-dependence of B_2 reflects a temperature-dependent pair interaction energy, w, we calculate w at the temperatures, at which B_2 data are available. To link B_2 and w, we approximate B_2 with the second osmotic virial coefficient and use[52]

$$B_2(T) = 12\int_0^\infty \left\{1 - \exp\left[-\frac{w(r)}{k_B T}\right]\right\}\tilde{r}^2 d\tilde{r} \qquad \tilde{r} = r/a \qquad (12)$$

For $w(r)$, we use the potential function introduced in ref 24

$$w(r) = \frac{4\epsilon}{\alpha^2}\left\{\frac{1}{[(r/a)^2 - 1]^6} - \alpha\frac{1}{[(r/a)^2 - 1]^3}\right\} \qquad (13)$$

because at $\alpha > 1$, its range is shorter than the molecular diameter a and a better fit to the protein intermolecular interactions. As in previous work,[24] we fixed α at 50 and assumed that it is independent of temperature.[24] From the value of B_2 at each temperature, we determined the potential depth, ϵ. We found that ϵ is a weak, roughly linear function of temperature, changing from $-4.84k_BT$ to $-4.66k_BT$ between 280 and 294 K. This weak dependence agrees with a previous conclusion that the temperature effects on the intermolecular interactions occur mainly through the Boltzmann factor, while hydration of the lysozyme molecules, etc., play a lesser role.[37]

The mean value of ϵ is $-4.75k_BT = -11.3$ kJ mol^{-1}. The near lack of temperature dependence suggests that the entropy contributions to the interaction potential are small, and ϵ is mostly enthalpic in nature. To compare ϵ with the enthalpy of crystallization, we scale ΔH_{crys} with one-half of the coordination number the crystal lattice $Z/2 = 3$ in the primitive tetragonal lattice of lysozyme.[36,53] We see that $2|\Delta H^\circ_{cryst}|/Z = 21.7$ kJ mol^{-1}, significantly higher than $|\epsilon|$. The energy ϵ is determined from B_2 data and is averaged over all of the polar angles. This comparison suggests that the interaction potential around the lysozyme molecules is anisotropic, and during crystallization, the deep minimums are indeed selected. Then, the similarity between ΔH_{L-H} and ΔH°_{cryst} suggests that in the dense liquid some of the deep minimums are also occupied; i.e., the dense liquid in lysozyme solutions is structured. Note that this ordering is not necessarily the same as in the crystal; it need not be compatible with a crystallographic symmetry group. This allows the dense liquid to find the deepest minimums and $|\Delta H_{L-H}|$ to reach values exceeding $|\Delta H^\circ_{cryst}|$.

Significance of the Higher-Order Virial Terms. Figure 6 compares the $\mu(\phi)$ dependencies at a fixed $T = 285$ K, calculated by neglecting higher-order terms in the virial-type expression to the full $\mu(\phi)$ from Figure 3. Similar relations between the truncated and the full $\mu(\phi)$'s were found at all temperatures within the T range of Figure 3. We see that the only approximation that relatively accurately predicts the compositions of the phases in L−L equilibrium is the one augmenting the CS expression for noninteracting hard spheres with an "attractive" second virial coefficient. The expressions that omit the volume occupied by the protein molecule are particularly inaccurate.

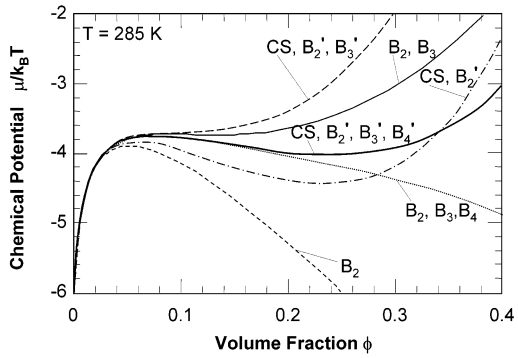

Figure 6. Illustration of the significance of the higher-order terms in the virial expansion of the chemical potential $\mu(\phi)$ at $T = 285$ K; $\mu(\phi)$ dependencies calculated with different approximations. Notation: CS $-\ln\phi - 3 + (3-\phi)/(1-\phi)^3$; $B_i' - i/i - 1\ B_i'\phi^{i-1}$, $B_i - (i/i-1)B_i\phi^{i-1}$. Thus, the thick solid curve was calculated allowing for all factors in $\mu(\phi)$ dependence discussed here. $\mu/k_BT = \ln\phi - 3 + (3-\phi)/(1-\phi)^3 + 2B_2'\phi + 3/2\ B_3'\phi^2 + 4/3\ B_4'\phi^3$.

This observation suggests that caution should be exercised when using the B_2 as a universal predictor of the phase behavior in protein solutions.[54,55] On the other hand, since the combination of B_2 with the excluded volume terms yields results closer to the full $\mu(\phi)$, we submit that the pair of parameters (v_p, B_2) could be a more accurate predictor of the phase behavior in protein solutions. The ratio B_2/B_2^{HS}, found to cluster in a narrow range for a variety of protein solution conditions[56] while advantageous to B_2 only, omits B_i^{HS} ($i > 2$).

Note that even the extended two-parameter criterion is necessarily limited. We surmise that proteins with structured potentials, with a series of minimums and maximums,[4] for which $w(r)$ contains significant entropy contributions, will not comply with it. A ready example is ferritin, which has a maximum in the interaction potential preceding the minimum near the molecular surface[57] and a significant entropy contribution to the crystallization driving force,[48] does not exhibit L−L separation, its solubility does not depend on temperature, and $|B_2|$ in crystallizing solutions is near 0.[58]

Conclusions and Perspectives for Future Work

We showed that data on the coexistence lines for liquid−liquid separation can be used to characterize the chemical potential and, hence, the activity of proteins in solutions with concentrations up to 320 mg mL^{-1} and likely higher at temperatures within and near the range in which L−L separation occurs.

We found that the enthalpy of liquid−liquid separation is comparable to the crystallization enthalpy. Arguments have been presented suggesting that this closeness is attributable to structuring of the dense liquid so that pairs of adjacent molecules occupy energetically favored sites in their pair interaction potential. Such structuring could have consequences for the biological functions of the proteins; it may also facilitate or hamper the formation of a consequent solid phase and merits experimental and theoretical tests.

We showed that exact accounting for the volume excluded by a molecule v_p based on the Carnahan−Starling expression combined with the second virial coefficient B_2 allows a reasonable prediction of the composition of the dense liquid phase, while the second virial coefficient by itself is misleading. This suggests that the pair (v_p, B_2) may be a better predictor of the phase behavior of proteins in solution, including their crystallizability. Future experimental work can focus on probing the applicability limits of this criterion by comparing the

predictions for a line of proteins with their actual phase behavior. Rationalization is more likely to come from numerical simulations, such as Monte Carlo, in which both the radial and angular dependencies of the interaction potentials are adjusted to experimentally determined facts about the system at hand.

Acknowledgment. We thank Neer Asherie, Anotoly B. Kolomeysky, Jianzhong Wu, Alexey Lomakin, Rhoda Elison Hirsch, and Qiuying Chen for many helpful suggestions on the manuscript. This work was supported by the Office of Biological and Physical Research, NASA (Grants NAG8 1824 and NAG8 1854) and the National Heart, Lung and Blood Institute, NIH (Grant HL 58038).

References and Notes

(1) Fulton, A. B. *Cell* **1982**, *30*, 345−347.
(2) Luby-Phelps, K. *Int. Rev. Cytol.* **2000**, *192*, 189−221.
(3) Fersht, A. *Structure and mechanism in protein science*; W. H. Freeman: New York, 1999.
(4) Leckband, D.; Israelachvili, J. *Q.. Rev. Biophys.* **2001**, *34*, 105−267.
(5) Wu, J.; Bratko, D.; Prausnitz, J. M. *Proc. Natl. Acad. Sci. U.S.A.* **1998**, *95*, 15169−15172.
(6) Kuehner, D. E.; Heyer, C.; Ramsch, C.; Fornefeld, U. M.; Blanch, H. W.; Prausnitz, J. M. *Biophys. J.* **1997**, *73*, 3211−3224.
(7) Johansson, H. O.; Brooks, D. E.; Haynes, C. A. *Int. Rev. Cytol.* **2000**, *192*, 155−170.
(8) Minton, A. P. *Curr. Opin. Biotechnol.* **1997**, *8*, 65−69.
(9) Bratko, D.; Chakraborty, A. K. *Phys. Rev. E: Stat. Phys., Plasmas, Fluids, Relat. Interdiscip. Top.* **1995**, *51*, 5805−5817.
(10) Bolen, D. W. *Methods Mol. Biol.* **2001**, *168*, 17−36.
(11) Lunelli, L.; Bucci, E.; Baldini, G. *Phys. Rev. Lett.* **1993**, *70*, 513−516.
(12) Tardieu, A.; Verge, A. L.; Malfois, M.; Bonnette, F.; Finet, S.; Ries-Kaut, M.; Belloni, L. *J. Cryst. Growth* **1999**, *196*, 193−203.
(13) Guo, B.; Kao, S.; McDonald, H.; Wilson, W. W.; Asanov, A.; Combs, L. L. *J. Cryst. Growth* **1999**, *196*, 424−433.
(14) Thomson, J. A.; Schurtenberger, P.; Thurston, G. M.; Benedek, G. B. *Proc. Natl. Acad. Sci. U.S.A.* **1987**, *84*, 7079−7083.
(15) Liu, C.; Asherie, N.; Lomakin, A.; Pande, J.; Ogun, O.; Benedek, G. B. *Proc. Natl. Acad. Sci. U.S.A.* **1996**, *93*, 377−382.
(16) Muschol, M.; Rosenberger, F. *J. Chem. Phys.* **1997**, *107*, 1953−1962.
(17) Galkin, O.; Chen, K.; Nagel, R. L.; Hirsch, R. E.; Vekilov, P. G. *Proc. Natl. Acad. Sci. U.S.A.* **2002**, *99*, 8479−8483.
(18) Prausnitz, J. M.; Lichtenthaler, R. N.; DeAzevedo, E. G. *Molecular Thermodynamics of Fluid-Phase Equililbria*; Prentice Hall: Upper Saddle River, NJ, 1999.
(19) Debenedetti, P. G. *Metastable Liquids*; Princeton University Press: Princeton, NJ, 1996.
(20) Peters, R. A. *Trans. Faraday Soc.* **1930**, *26*, 797−809.
(21) Pagliaro, L. *Int. Rev. Cytol.* **2000**, *192*, 303−318.
(22) Walter, H.; Brooks, D. E. *FEBS Lett.* **1995**, *361*, 135−139.
(23) Walter, H. *Int. Rev. Cytol.* **2000**, *192*, 331−343.
(24) ten Wolde, P. R.; Frenkel, D. *Science* **1997**, *277*, 1975−1978.
(25) Talanquer, V.; Oxtoby, D. W. *J. Chem. Phys.* **1998**, *109*, 223−227.
(26) Galkin, O.; Vekilov, P. G. *Proc. Natl. Acad. Sci. U.S.A.* **2000**, *97*, 6277−6281.
(27) Eaton, W. A.; Hofrichter, J. In *Advances in Protein Chemistry*; Anfinsen, C. B., Edsal, J. T., Richards, F. M., Eisenberg, D. S., Eds.; Academic Press: San Diego, 1990; Vol. 40, pp 63−279.
(28) Benedek, G. B.; Pande, J.; Thurston, G. M.; Clark, J. I. *Prog. Retinal Eye Res.* **1999**, *18*, 391−402.
(29) Lomakin, A.; Chung, D. S.; Benedek, G. B.; Kirschner, D. A.; Teplow, D. B. *Proc. Natl. Acad. Sci. U.S.A.* **1996**, *93*, 1125−1129.
(30) Koo, E. H.; Lansbury, P. T., Jr.; Kelly, J. W. *Proc. Natl. Acad. Sci. U.S.A.* **1999**, *96*, 9989−9990.
(31) Hagen, M. H. J.; Frenkel, D. *J. Chem. Phys.* **1994**, *101*, 4093−4097.
(32) Chu, B. *Laser Light Scattering*, 2nd ed.; Academic Press: New York, 1991.
(33) Muschol, M.; Rosenberger, F. *J. Chem. Phys.* **1995**, *103*, 10424−10432.
(34) Grigsby, J. J.; Blanch, H. W.; Prausnitz, J. M. *Biophys. Chem.* **2001**, *91*, 231−243.
(35) Petsev, D. N.; Thomas, B. R.; Yau, S.-T.; Vekilov, P. G. *Biophys. J.* **2000**, *78*, 2060−2069.
(36) Steinrauf, L. K. *Acta Crystallogr.* **1959**, *12*, 77−78.
(37) Piazza, R.; Peyre, V.; Degiorgio, V. *Phys. Rev. E: Stat. Phys., Plasmas, Fluids, Relat. Interdiscip. Top.* **1998**, *58*, R2733−R2736.
(38) Cacioppo, E.; Munson, S.; Pusey, M. L. *J. Cryst. Growth* **1991**, *110*, 66−71.
(39) Rosenberger, F.; Howard, S. B.; Sowers, J. W.; Nyce, T. A. *J. Cryst. Growth* **1993**, *129*, 1−12.
(40) Stanley, H. E. *Critical Phenomena and Phase Transitions*; Oxford Science Publishers: New York, 1971.
(41) Carnahan, N. F.; Starling, K. E. *J. Chem. Phys.* **1969**, *51*, 635−636.
(42) Lomakin, A.; Asherie, N.; Benedek, G. B. *J. Chem. Phys.* **1996**, *104*, 1646−1656.
(43) Binder, K.; Fratzl, P. In *Phase Transformation in Materials*; Kostorz, G., Ed.; Wiley: New York, 2001.
(44) Cahn, J. W.; Hilliard, J. E. *J. Chem. Phys.* **1958**, *28*, 258−267.
(45) Casselyn, M.; Perez, J.; Tardieu, A.; Vachette, P.; Witz, J.; Delacroix, H. *Acta Crystallogr., Sect. D* **2001**, *57*, 1799−1812.
(46) Atkins, P. *Physical Chemistry*, 6th ed.; Freeman: New York, 1998.
(47) Cacioppo, E.; Pusey, M. L. *J. Cryst. Growth* **1991**, *114*, 286−292.
(48) Vekilov, P. G.; Feeling-Taylor, A. R.; Yau, S.-T.; Petsev, D. N. *Acta Crystallogr., Sect. D* **2002**, *58*, 1611−1616.
(49) Gray, R. J.; Hu, W. B.; Kudryavtsev, A. B.; Delucas, L. J. *J. Cryst. Growth* **2001**, *232*, 10−16.
(50) Schall, C.; Arnold, E.; Wiencek, J. M. *J. Cryst. Growth* **1996**, *165*.
(51) Lomakin, A.; Asherie, N.; Benedek, G. *Proc. Natl. Acad. Sci. U.S.A.* **1999**, *96*, 9465−9468.
(52) Hill, T. L. *Introduction to Statistical Thermodynamics*; Dover: New York, 1986.
(53) Vaney, M. C.; Maignan, S.; Ries-Kaut, M.; Ducuix, A. *Acta Crystallogr., Sect. D* **1996**, *52*, 505−517.
(54) George, A.; Wilson, W. W. *Acta Crystallogr., Sect. D* **1994**, *50*, 361−365.
(55) Rosenbaum, D. F.; Zamora, P. C.; Zukoski, C. F. *Phys. Rev. Lett.* **1996**, *76*, 150−153.
(56) Rosenbaum, D. F.; Kulkarni, A.; Ramakrishnan, S.; Zukoski, C. F. *J. Chem. Phys.* **1999**, *111*, 9882−9890.
(57) Petsev, D. N.; Vekilov, P. G. *Phys. Rev. Lett.* **2000**, *84*, 1339−1342.
(58) Yau, S.-T.; Petsev, D. N.; Thomas, B. R.; Vekilov, P. G. *J. Mol. Biol.* **2000**, *303*, 667−678.